Thermochimica Acta, 29 (1979) 41–56

AUTOMATION OF FACTOR-JUMP THERMOGRAVIMETRY FOR ACTIVE COMPUTER CONTROL

B. DICKENS
Center for Materials Research, National Bureau of Standards, Washington, D.C. 20234 (U.S.A.)
(Received 9 February 1978)

ABSTRACT

A scheme of automation of a thermogravimetry apparatus is described which was developed with the factor-jump method in mind. Temperature, pressure and flow rates of two gases are controlled; all components except the furnace are commercially available. This paper describes the details of the automation scheme and provides data on the quality of its performance. The scheme includes a mini-computer; if no feedback is required, a recording computer terminal can be used instead.

INTRODUCTION

This paper documents the details and performance of automation designed to implement "factor-jump" thermogravimetry[1]. An overview of the scheme has been given in ref. 2.

In its simplest form, factor-jump thermogravimetry consists of subjecting a sample to a series of plateaus in temperature, during each of which the weight loss of the sample is recorded continually. The trends of temperature and weight with time are then extrapolated to a common time, between the ending of one plateau and the beginning of the next, to give temperature, weight and rate of weight loss values of T_1, w_1, r_1 for the first plateau, and T_2, w_2, r_2 for the second. The quantities T_1, w_1 and r_1 are the values obtained when the sample has been kept at temperature T_1; similarly, the quantities T_2, w_2 and r_2 are the values obtained when the sample has been kept at temperature T_2. These quantities, the gas constant R, and the Arrhenius equation $r = Ae^{-E/RT}$ are used to provide an activation energy

$$E_i = R \frac{(T_1 T_2)}{(T_1 - T_2)} \ln (r_1/r_2) \qquad (1)$$

at time t_i, or extent of reaction C_i. Up to $\sim$ 30 activation energies may be obtained from one sample.

Thermogravimetry was chosen for the first implementation of the factor-jump method because it is a simple technique which provides kinetic information on the degradation of both soluble and insoluble samples in any condensed form, including,

for example, such specialized forms as foams. The factor-jump method was devised to enable us to take advantage of several aspects: (i) only one sample is used so that comparison between two samples with disparate thermal histories is avoided, (ii) no long extrapolation over atypical regions to initial rates is necessary, (iii) the initial and final sample weights are not needed to calculate an activation energy (although they are needed to relate the activation energy to a "degree of conversion" or "extent of reaction"), (iv) the extent of dominance of a particular combination of processes, as indicated by the consistency of their overall activation energy, can be explored over the course of the experiment or over a wide range of conditions and, conversely, (v) the weight-loss reactions can be studied under a narrow range of conditions, especially in temperature, simply by alternating between the two sets of condition-specifying values.

The repeated changing of conditions in the factor-jump method suggests a need for automation. The pros and cons of experiment automation and computerization have been debated many times. Here we summarize a few pertinent points. Because of their complexity, automated experiments are often difficult to assemble, troubleshoot and repair. The increased performance brings new problems previously either insignificant, unknown or ignored, and the warranties, guarantees and length of periods of sustained high performance in state-of-the-art equipment are strikingly short. The equipment is expensive but may be worthwhile if it enables measurements to be made more precisely, faster or for the first time. One problem with this kind of approach is that it is very difficult to make corrections in a pre-conceived fashion for some discontinuity in the data which is sometimes obvious to the eye. Also, the designer will often notice that only he can or wants to operate his creation.

Among the advantages of experiment automation, even without computer control, are the facts that the data can easily be read and stored, digital information is available for further machine processing, the apparatus can operate with a greater attention span while committing few or no transcribing errors, and operator errors are fewer because the operator has less to do. In general, the machine will have a quicker, more sustained response and will be able to use a standardized procedure to control, vary and read many factors probably with higher precision and with signal-averaging reiteration if necessary to improve signal-to-noise ratios. Measurements to constant precision can provide a performance uniform throughout the experiment. Also, one intends that the productivity and/or precision will be increased.

The disadvantages of computer-controlled automation are that programming is very time consuming (up to 90% of the total cost), the programs are rarely bug-free and the additional computer equipment seems expensive in absolute terms although mini-computers are actually remarkably inexpensive. The advantages of computer control include: essentially no computational mistakes are made (other than those resulting from errors in programming logic), estimates of precision become more tractable, measurements can be obtained to constant precision via feedback, and derived quantities can often be calculated in real time and their precision estimated so that the performance can be easily monitored and modified to be more uniform

during the experiment. Complex procedures become feasible and the experimental procedure becomes flexible.

The limits become those of money for the equipment, and of available time in manhours for the set-up and in real-time in the computer. What cannot be done quickly enough or is not important enough to do in real-time by computation must in a prototype instrument be delegated to an analog circuit. In mass-produced instruments, one can imagine locally autonomous microprocessors becoming feasible. In selecting our automation scheme, we have steered a middle course among competing philosophies, believing that a good laboratory automation system should be able to control perhaps 80% of the experiment without the aid of the mini-computer, that computers should be used for high speed computation and decision-making as well as for data acquisition and sequential control, and the system should, to some extent, be capable of running passively without a computer.

The scheme described here is the result of our intention to refine the automation and the procedure to reasonable limits. We kept in mind the possibility that, if those limits proved to not be very far, some or all of the automation should be capable of being used to better advantage with some other technique.

This publication documents the choice, assembly and performance of the hardware of our thermogravimetry automation. There has been some compromise between ease and elegance. The details of the computer programs which operate the apparatus in the factor-jump mode are given in refs. 3 and 4. Some experimental results are given in ref. 5. A user's manual is being written[6].

OVERALL DESCRIPTION OF AUTOMATION SCHEME

Our automation scheme provides a method of measuring the sample weight and also provides control of sample temperature, flow rate of N_2 and O_2 over the sample, and the pressure in the sample chamber. Although experiments with controlled humidity have not yet been carried out, saturated salt solutions could be used to generate a stream of gas with given moisture content to pass over the sample.

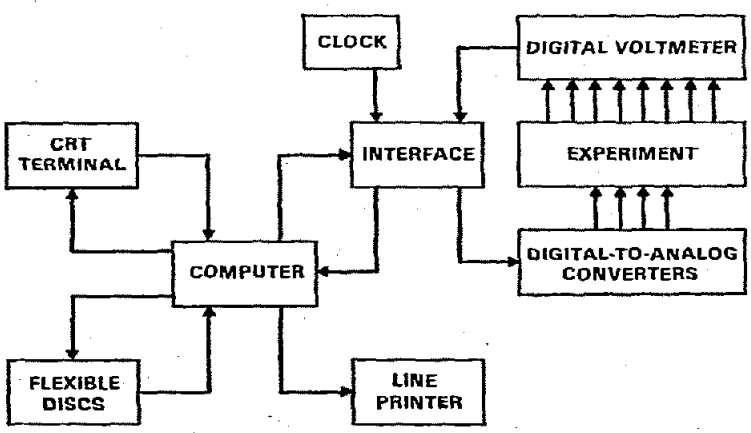

Fig. 1. A generalized, block-diagram outline of the factor-jump thermogravimetry apparatus.

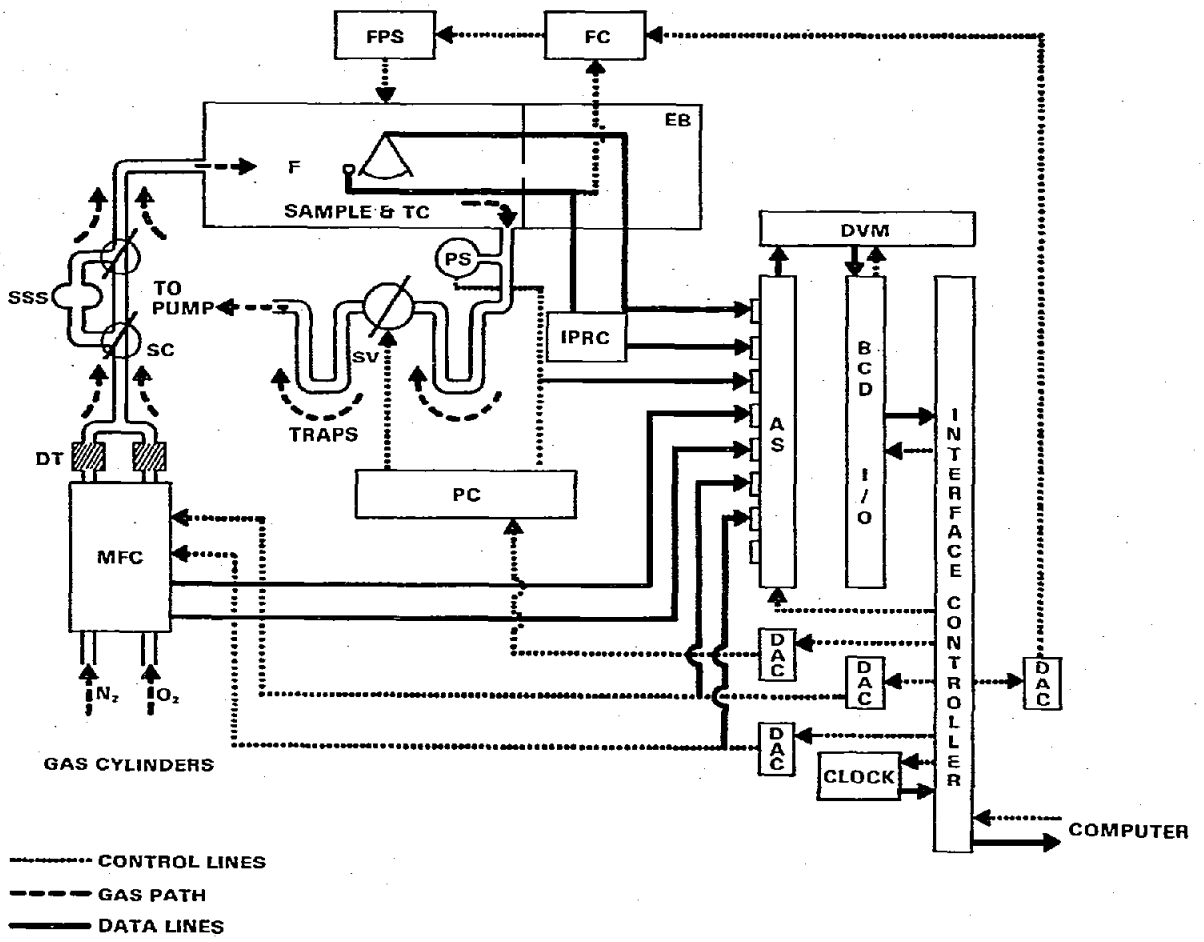

Fig. 2. The linkage between the controller and the experiment. Abbreviations used: AS, analog scanner; BCD I/O, digital input/output; DAC, digital to analog converter; DT, drying tubes; DVM, digital voltmeter; EB, electrobalance; F, furnace; FC, furnace controller; FPS, furnace power supply; IPRC, ice point reference cell; MFC, mass flow controller; PC, pressure controller; PS, pressure sensor; SC, stop-cock; SSS, saturated salt solution; SV, servo-driven valve; TC, thermocouple.

The general scheme is given in Fig. 1; all modules except the furnace are commercially available. The computer sends commands to the interface, which generates voltages used to specify the temperature, pressure and flow rates around the sample. The interface also reads voltages generated by the apparatus. The programs and data are stored on flexible diskettes and the progress of the experiment is displayed on the cathode ray tube computer terminal and recorded on the line-printer or on a diskette.

AUTOMATION DETAILS

Figure 2 shows the automation in more detail. These items will now be described.

Electrobalance

The electrobalance is a slightly modified version of a commercially available

horizontal-beam model. The original furnace has been replaced (see below) and the direction of gas flow is now over the sample towards the balance housing instead of the reverse. The thermocouple leads are brought out through the aperture in the balance housing originally intended for inlet of gas. In this way, the thermocouple leads are kept separate from the electrical leads and changeover from the thermocouple materials to copper wiring is accomplished in an electrically maintained ice point reference cell rather than in the balance housing (which may be warmed slightly as the attached furnace heats up). An inlet for a gas stream to introduce a back-pressure in the balance housing may be provided in the glass envelope surrounding the counter-weight arm/photocell mechanisms. So far we have not found this to be necessary.

Examination of the electrical weight signal from the electrobalance with an oscilloscope revealed tremendous sensitivity to room vibration and footfalls. This was reduced to an acceptable level ($\sim$ 20 μV) by (a) operating with a time constant of 5 sec, (b) using the balance on top of a thick heavy concrete slab on a sturdy table, and (c) installing a 1/4-in square of a shock absorbing rubber material under each of the table legs.

There is some drift in the electrobalance readings. This drift in the instrument will be included in the apparent rate of weight loss, which must be kept large enough to swamp out the effect of the drift. The balance takes several hours to settle down to a minimum drift, the final value of which varies with the time constant used. Further, there is trouble in obtaining reproducible weighings. These facts introduce problems into the determination of the initial and final weights of the sample, and thus complicate operation in the two-sample method, where rates in the two samples must be related to the extent of conversion (or reaction) via the initial, final and current weights before an activation energy can be calculated. In the factor-jump method, an activation energy is calculated from extrapolations in the rate of change of the current weight at different temperatures; knowledge of the initial and final weights is only of interest in relating an activation energy to the extent of reaction at which it was determined. Because the activation energy is usually a slowly changing parameter, this limitation is only slight.

The sample is placed at the end of a horizontal balance arm, only part of which is in the furnace. Our first prototypical design of the reaction manifold housing the furnace and the balance arm inadvertently placed the expansion/contraction mechanism outside the furnace and thus rendered it ineffective. A change in temperature of 100°C produced changes of up to 100 μV in the voltage representing the apparent sample weight. In vacuum, these changes took 7–8 min to decrease to level of the noise ($\sim$ 20 μV). A redesigned reaction manifold placed the expansion mechanism in the furnace but there are still noticeable changes of apparent sample weight with temperature.

We examined the size of the arm expansion effect in our apparatus. The arm was allowed to equilibrate at the temperatures employed. The effect of changing the length of the balance arm is to change the apparent rate of weight loss, r. If $r = k\mathrm{d}w'/\mathrm{d}t$, where $\mathrm{d}w'/\mathrm{d}t$ is the real rate of weight loss, then substitution in eqn. (1)

shows that the apparent activation energy, E, and the real activation energy, E', are related by

$$E = \frac{RT_1T_2}{\Delta T} \ln\left(\frac{r_1}{r_2}\right)$$

$$= \frac{RT_1T_2}{\Delta T} \ln\left(\frac{dw_1'}{dt}\frac{dt}{dw_2'}\right) + \frac{RT_1T_2}{\Delta T} \ln\left(\frac{k_1}{k_2}\right)$$

$$= E' + \frac{RT_1T_2}{\Delta T} \ln\frac{k_1}{k_2}$$

The dependence of k on temperature was determined by monitoring the weight of a piece of non-magnetic wire in the sample pan. The largest effect occurred around 250°C, where a 15°C change in temperature produced a change of 0.1% in sample weight. This introduces a correction term of $\sim(2 \times 250 \times 250/15)\ln(1.001/1.000)$ $\sim$ 8 cal mole^{-1}, which is negligibly small.

In practice, therefore, the effect of arm expansion is negligible in our application of the factor-jump method because we operate with small ($\leq$ 15°C) temperature jumps. These small jumps are required to keep the rates of weight loss within reasonable bounds[5]. To subdue the effect of slow changes in the balance arm, we allow an equilibration period, and force the degradation to occur above a minimum rate of weight loss.

In those cases where much larger temperature jumps are necessary (i.e., for very small activation energies or very high temperatures) it may be necessary to cancel out arm expansion effects by mathematical computation. The effect of balance arm expansion is to increase the apparent sample weight and hence the observed rate of weight loss. If the sample weight is w, the apparent weight of the bucket and arm assembly is b, the electronic suppression applied to the electrobalance signal is s, and the effective weight of the counterweight is c, then the apparent sample weight a_1 for a given balance arm extension k_1 is given by

$$a_1 = k_1(w + b) - s - c$$

and the apparent rate of weight loss is given by $da_1/dt = k_1(dw/dt)$. The effect of balance arm expansion could be cancelled out by multiplying the ratio of apparent rates, da_1/dt and da_2/dt, by k_2/k_1.

The quantity k_2/k_1 can be estimated from the relationship

$$\frac{a_1 + s + c}{a_2 + s + c} = \frac{k_1(w_1 + b)}{k_2(w_2 + b)} = \frac{k_1}{k_2}, \text{ when } w_1 = w_2$$

The quantities s, c, and b are all experimental constants. Because diffusion processes in the sample are usually not of interest and must be minimized, the sample weight cannot be large. However, the weight of the bucket can easily be many times that of the sample. A heavy bucket magnified changes in length of the balance arm and

produces discernable corresponding changes in the apparent sample weight. (It also increases the counterweights or suppression needed and forces the balance to operate near the limit of its specifications). The apparent sample weights a_1 and a_2 can be estimated from extrapolation of the polynomials fitting the sample weight/time trend in adjacent plateaus to a time between the two plateaus. There will be some error in these estimates because the first half of the inter-plateau region will be assumed to behave like the first plateau and the second half like the second plateau even though there was in fact a gradual transition between the two plateaus. At a given time, $w_1 = w_2$ for the instantaneous sample weights. Therefore, k_1 and k_2 could be estimated during the experiment from the ratio $(a_1 + s + c)/(a_2 + s + c)$ and applied as a corrective term to the ratio of rates of weight loss used in eqn. (1). The same process would allow corrections for buoyancy effects. Indeed the effects of balance arm expansion and changes in atmospheric density would be inseparable under normal operating conditions. The buoyancy effect above could be studied by changing the pressure rather than the temperature. However, up to now we have not found it necessary to incorporate this procedure into our program.

Furnace

The furnace supplied by the manufacturer of the thermobalance is far too massive for our needs. In particular it takes at least 5 min to cool the 10–15 °C difference in temperature used between adjacent isothermal regions and takes even longer to stabilize at the new temperature. We therefore designed a rapid-response furnace

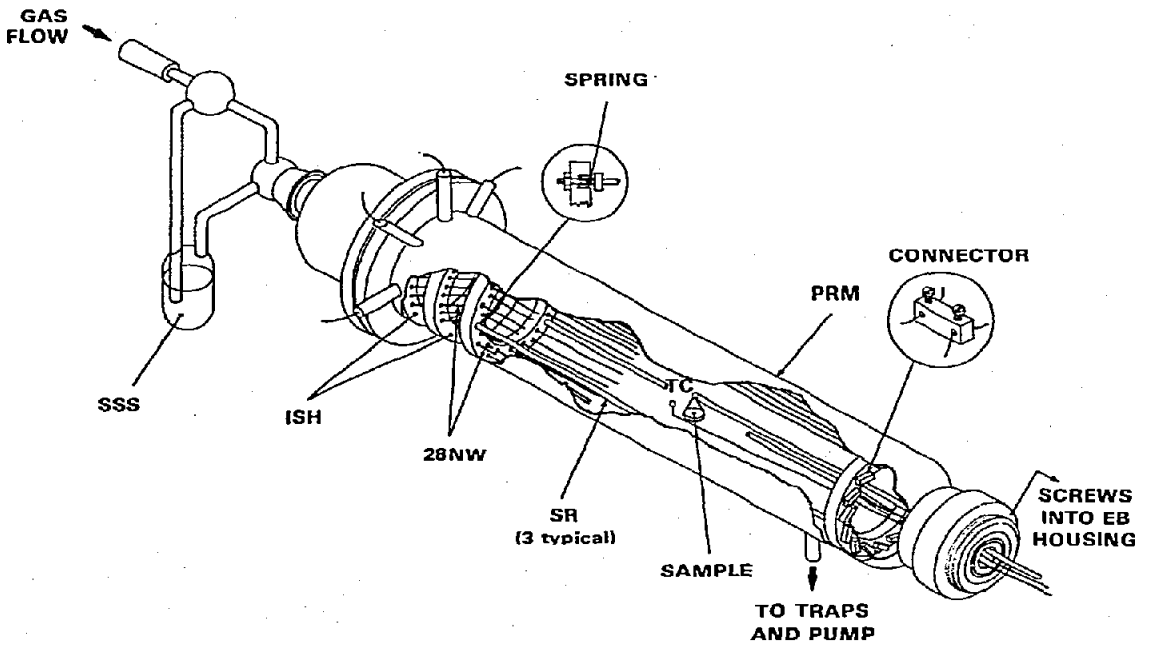

Fig. 3. A rapid response furnace featuring in-stream heaters for the gas stream (flow is left to right). Abbreviations used: 28 NW, 28 gauge nichrome wire; EB, electrobalance; ISH, in-stream heater; PRM, pyrex reaction manifold; SR, support rod; SSS, saturated salt solution.

(Fig. 3) which uses many strands of bare nichrome wire strung between circular forms to heat the sample environment. For applications where a flowing gas stream is used, an additional heater heats the gas stream throughout its entire cross-section, thus avoiding the common practice of heating the stream only at its edge. To include the gas stream heater, we had to reverse the direction of gas flow, which now enters on the side of the sample remote from the balance housing and exits before the balance housing through a tube in the borosilicate reaction manifold.

The circular forms in the main heater are 22 mm i.d., 36 mm o.d. and 3 mm thick rings made from a machinable ceramic. The outside ends are held 10 cm apart by three 1.5-mm threaded stainless steel rods. At the end of each rod there is an Inconel spring, which, in theory, is supposed to force the furnace to expand lengthwise to take up slack in the nichrome heating wires as they expand on heating. In practice, our present springs are not strong enough, but fortunately the expansion of the heater wires does not appear to be troublesome. Taut heater wires would probably improve the temperature homogeneity in the furnace, but that is currently within acceptable limits (see later). To put 30 strands of 28 gauge nichrome in the furnace, it was necessary to string the heater wires in two circles. Each wire passes through the furnace three times and then is joined to its neighbor in series with a small specially machined stainless steel connector with two lock screws. The sample heater has a resistance of 36 Ω.

The gas stream heater consists of two machinable ceramic circular forms each with 7 parallel strings of 28 gauge nichrome wire with a total resistance of ~ 20 Ω. Its diameter is the same as that of the main heater. The main and gas stream heaters are connected in series to give a total heater resistance of ~ 56 Ω.

The heaters are contained in a pyrex reaction manifold (Fig. 3) which attaches to the balance housing at one end and has a flange at the other to provide a connection to allow removal of the electrical heaters. Electrical leads are introduced into the manifold through small pyrex tubes sealed with high-temperature cement subsequently coated with hot wax. The pyrex manifold has been coated with platinum paint inside and out to improve the temperature homogeneity. Our initial design included a 1-cm diameter clear spot in the platinum coating to provide a viewing port. This was located on the balance side of the sample; after prolonged use it became obscured by degradation products. Later versions have no viewing port.

Temperature controller

The temperature controller is a current-adjusting type, with a "soft" manual station and provisions for the proportional, reset, rate and approach modes of control. The target temperature is specified by a 0–10 V d.c. remotely originating high level input which is divided by a suitable external combination of resistors (100 Ω/25 kΩ) from 10 V d.c. to 0.040 V d.c. This corresponds to a type-E thermocouple voltage of 537 °C, near the strain point of the borosilicate reaction manifold. With the high-level input at 0 V d.c. and the thermocouple connections shorted out, there as a small residual deflection of the deviation meter; we were fortunate in that this could

be removed conveniently by setting an appropriate but low figure on the "local" set-point, a 4-digit thumb wheel-driven potentiometer calibrated for 0–10 mv. This merely introduces a small positive bias voltage into the control loop.

The 0–5-mA current output of the controller is sent across an externally supplied 2 kΩ resistor to provide a reference signal of 0–10 V d.c. In practice, several external resistances ranging from 100 Ω to 20 kΩ have been mounted on a rotary switch but so far only the 2 kΩ resistor has been used. This 0–10 V d.c. signal is used to program a d.c. power supply attached to the furnace. It was found that the proportional term k_1 in the correction signal[7, 8]

$$S = -\left(k_1\theta + k_2 \int_{\varepsilon-\tau}^{\varepsilon} \theta \mathrm{d}t + k_3 \frac{\mathrm{d}\theta}{\mathrm{d}t}\right)$$

was too large with the proportional band width at 200 °C to allow non-zero settings for reset, k_2, and rate, k_3, (the variable θ represents the difference between specified and actual temperature, t is time and τ is the reset integration time). We increased the proportional range (and thus decreased k_1) tenfold by installing a 100-kΩ resistor in the control amplifier section of the temperature controller. After a brief flirtation with a general method[8] of estimating optimum settings, we chose the settings heuristically. The general philosophy was to remove excessive overshoot, which would "burn off" our polymer sample, yet approach the target temperature reasonably quickly, to remove all offsets so that we reached the target value every time and to reduce wanderings in temperature during the temperature plateaus. Approach was set to be 180 °C (90% of maximum) to reduce overshoot. The value of k_2 (reset) was set at the maximum so that slowly changing offsets from the actual target value of temperature would not occur. Overall rate of attainment of the target temperature value was strongly dependent on k_1, which has to be made as large as possible (i.e., a small setting on the proportional set screw) with the reset value at maximum. The final value of k_1 was chosen solely on the criterion of steadiest temperature during the isothermal sections. The contribution of the rate (k_3) was finally set to zero; this seemed to give the greatest stability in the temperature control. These settings were determined by operating the furnace in a vacuum, the worst condition for temperature control.

Any oscillation in the temperature appears in magnified form in the sample weight/time data and complicates the fitting of these data by a polynomial. The weight–time polynomial is of critical importance because it must be extrapolated and differentiated[4] to give a rate of weight loss to be used in eqn. (1).

Furnace power supply

Power is supplied to the furnace by a programmable power supply which has maximum outputs of 100 V d.c. and 2.5 A. The output voltage, $E_0 = -E_p R_r/R_p$, depends on the programming voltage, E_p, and programming resistance, R_p, (external

to the power supply) as well as the reference resistance, R_r, (inside the power supply).

In our application, the low-level lead of the 0–10 V d.c. signal from the 2-kΩ resistor/temperature controller circuitry is connected directly to the appropriate power supply terminal. The high-level lead is attached to the power supply across a 2 kΩ resistor (i.e., R_p). Because $E_p \leq 10$ V d.c., $R_p = 2$ kΩ and $R_r = 15$ kΩ (as wired in the power supply at the factory)

$$E_0 \leq -10(15/2) = 75 \text{ V d.c.}$$

The actual current sent through the furnace depends on the furnace resistance and on the front panel settings of the limits on output current and voltage from the power supply, but typical maximum values used are 75 V d.c. and 1.5 A which provide ~ 110 W of heating power. Both current and voltage outputs are displayed on meters. This has been found to be extremely convenient for monitoring the functioning of the temperature-control network.

Performance of the temperature-control network

For minimum extrapolation time in the factor-jump method, the furnace should respond rapidly to programmed temperature changes and should quickly settle down to a stable temperature very close to that programmed. The furnace should also provide a satisfactorily homogeneous temperature distribution about the sample.

The dynamic performance of the furnace is illustrated in Fig. 4. Thus in the regions of interest (150–350 °C) the furnace heats up at rates of 20 to 12 °C sec^{-1}, and

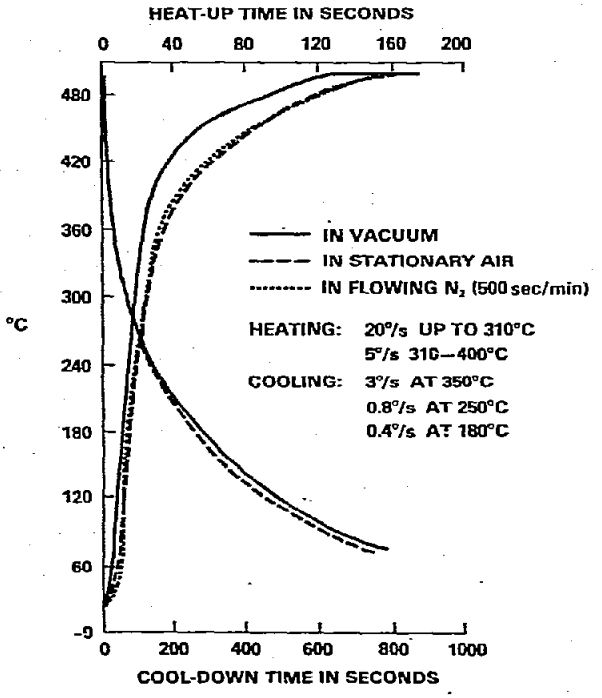

Fig. 4. Heating and cooling of rapid response heater.

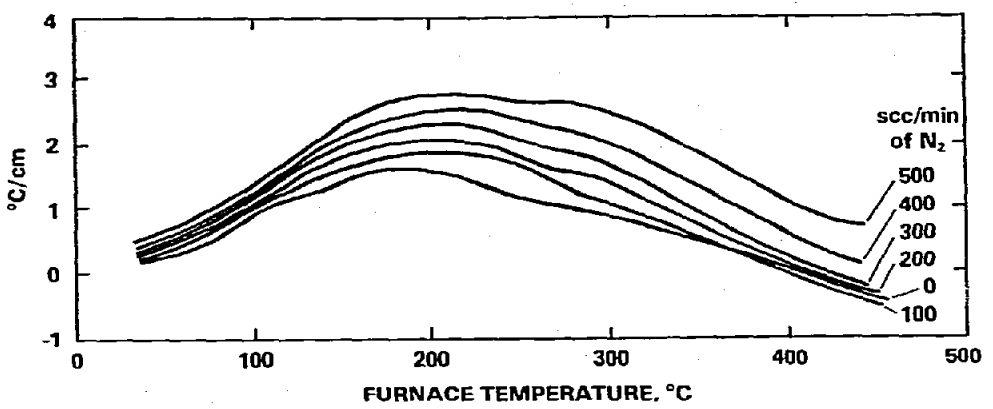

Fig. 5. Temperature homogeneity along axis of cylindrical rapid response furnace at various flow rates in scc min^{-1}. Temperature gradient obtained from two thermocouples spaced about sample position. Pressure = 1 atm.

cools down at rates of 3 to 0.3 °C sec^{-1}. The longest equilibration time will occur at a jump from 165 to 150°C; this causes a non-equilibrium condition gap of ~ 40 sec to exist between plateaus. At the high end of the operating temperature range a 15°C change in temperature will cause a gap of only 4 sec. The furnace steadies down to a stable value of ± 0.15°C in vacuum and ± 0.05°C at atmospheric pressure.

Temperature homogeneity was estimated by measuring the e.m.f.'s of three type-E thermocouples placed about the sample position. Figure 5 shows the homogeneity as a function of flow and temperature.

The following argument estimates limits on the acceptable offset between the real temperature of the sample and the value measured by the thermocouple. Suppose that the activation energy, E, is given by eqn. (1); also, suppose that the apparent temperatures, T, are related to the real temperatures T' by an offset T_0. Then the real activation energy, E', is given by

$$E' = \frac{R(T_1 - T_0)(T_2 - T_0)}{\Delta T} \ln (r_1/r_2)$$

$$= \left(\frac{R}{\Delta T} \ln \frac{r_1}{r_2}\right)(T_1^2 - 2T_1T_0 + T_0^2), \text{ if } T_1 \sim T_2$$

$$= E + \frac{2ET_0}{T_1} + \frac{T_0^2E}{T_1^2}$$

$$= E + \frac{2ET_0}{T_1}, \text{ if } T_0 \ll T_1, T_2$$

$$= E + \Delta E$$

where E is the calculated activation energy. The fractional error in E' is given approximately by $2T_0/T_1$, which. for $T \sim 500$ K and an error of 1 % in E allows a temperature

offset of 2.5°C. For a more generous error of 1 kcal in an activation energy of 30 kcal $mole^{-1}$, the tolerable temperature offset at 500 K is 500/60 ~ 8.3°C.

This surprisingly large offset may be viewed in two ways: (i) the thermocouple need not be inconveniently close to the sample, and (ii) appreciable furnace inhomogeneity can be tolerated. We placed the thermocouple as near to the sample cup as is convenient (< 2 mm from the upstream end), and, at our maximum inhomogeneity of 3° cm^{-1}, expect a maximum temperature offset of ~ 1.5° between the thermocouple and the middle of the sample cup. This would introduce maximum errors of 0.6% (= 2 × 1.5 × 100/450) to 0.5% (= 2 × 1.5 × 100/640) into the calculated values of E at 450 and 600 K.

Pressure measurement

The "absolute" pressure in the reaction manifold is measured by a capacitance-type pressure sensor which references the actual pressure in the reaction manifold to the pressure in an internal evacuated compartment. The measurement is conditioned by an electronics unit into a 0–10 V d.c. signal linear over the range 0–1000 mm Hg and is displayed on a 4–1/2 place digit readout. The zero of pressure on the sensor depends to some extent on the orientation of the sensor and perhaps on shocks received by the sensor. The zero of the sensor is adjusted frequently by reference to a McLeod gauge.

Pressure control

Provided there is a flow of gas, the pressure in the system is controlled by a servo-driven bakeable valve on the exhaust, i.e. just before the vacuum pump. This type of valve is normally used on gas input lines and, in order to use it in the exhaust line, we had to modify the valve controller module. The valve cable and signal light connections were changed so that all "input" connections were actually connected to the corresponding output connections, and vice versa. "Opening" and "closing" labels on the front panel were also interchanged. The controller receives a 0–10 V d.c. signal from the pressure measuring system and compares it with a remotely originating 0–10 V d.c. signal. If the pressure signal is the greater, the controller sends pulses to open the valve (as delivered, the controller would have closed the valve). If the pressure signal is the lesser, the exhaust valve is closed.

Because the pressure sensor provides a change of only 0.01 V d.c. per mm Hg, the system as initially assembled required an extremely large deviation from the set point before it would respond. This situation was corrected by increasing the gain of the deviation amplifier in the valve controller (the feedback resistor was changed from 27 kΩ to 1 kΩ).

Both the pressure sensor and the exhaust valve can be baked to try to remove deposits. To reduce this maintenance to a minimum, we have separated the pressure sensor from the exhaust stream by ~ 10 cm of tubing (Fig. 2). However, we placed the sensor near the exhaust valve (downstream from the sample) to maximize the efficacy of pressure control. Operation in this position has been satisfactory. We have

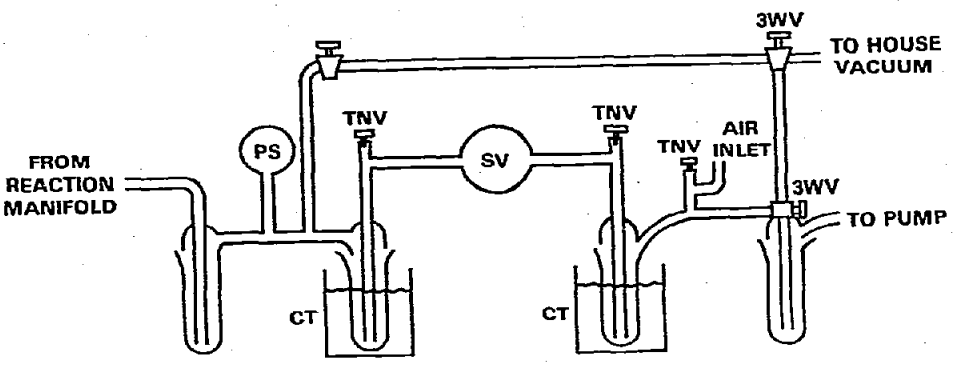

Fig. 6. Exhaust system. Abbreviations used: 3 WV, 3-way valve; CT, cold trap; PS, pressure sensor; SV, servo-driven valve; TNV, teflon needle valve.

placed traps on either side of the exhaust valve (Fig. 6). When running experiments under a vacuum, we bypass the exhaust valve entirely, thus improving the conductance of the system.

Gas flow control

Gas flow in two lines is controlled by a two-channel mass flow controller, slightly modified to our requirements by the supplier. As supplied off-the-shelf, the flow controller was programmable manually by adjusting two front panel potentiometers to give 0–5 V d.c. signals to specify each flow. Our instrument is calibrated for mass flows of 0–500 scc min^{-1} N_2 on channel 1 and 0–200 scc min^{-1} on channel 2. It also has factory-installed mini-plug inputs for remote programming of the flows and outputs making available 0–5 V d.c. voltages indicating the actual flow in each channel. Each gas line contains a drying cartridge between the gas cylinder and the flow controller. The flows are essentially constant at all useful pressures and the accuracy is within 1% of full scale.

TABLE 1

PERFORMANCE OF PRESSURE CONTROLLER AT VARIOUS FLOW RATES

Pressure (mm Hg)	*Flow (scc min^{-1} N_2)*					
	500	*250*	*100*	*75*	*50*	*25*
760[a]	758(1)	762(1)	759(1)	759(2)	758(4)	760(2)
400[a]	400.7(2)	402(1)	400(2)	400(2)	400(2)	397(5)
200[a]	200(3)	201.4(1)	200(3)	201(1)	201(2)	201(2)
100[b]	101.6(1)	101.5(1)	101.2(1)	101.6(1)	100.3(8)	100(1)

[a] House vacuum (125–165 mm Hg) on exhaust.
[b] Vacuum pump on exhaust.
Numbers in parentheses are the standard deviations in the last digit given.

Performance of pressure control

Tests were conducted to determine the precision of pressure control at several pressures and flow rates. The results, given in Table 1, show adequate control at all reasonable levels. The equilibration time to achieve the final level of control depends on the pressure, the flow rate, and the starting position of the servo-driver exhaust valve. A really bad case (e.g., 760 mm Hg and 25 scc min^{-1} N_2 with the valve opening far from the final setting) can take up to 1000 sec to steady down unaided, but the valve can be set using the manual option on the controller within 30 sec. The response time of the pressure/flow system to reasonably small changes under realistic conditions is much less than the 150–200 sec equilibration time usually allowed in our programmed application of the factor-jump technique. In most cases control at the new levels can be achieved within 30 sec. This is clearly adequate for our purposes.

Interface between computer and experiment

In specifying an interface to allow two-way communication between computer and experiment, we purposely stayed on the side of generality. The MIDAS* interface[9] allows experiment automation in a speedy, convenient fashion using any device which generates and receives ASCII commands, i.e., a teletype, a magnetic cartridge terminal or a computer. In gaining convenience, however, one sacrifices elegance and some operational speed, for the MIDAS interface has no interrupts, operates in a sequential mode in that only one component module can be addressed at a time, and processes commands and provides data serially, i.e., character by character.

In addition to the crate, power supply and command modules, the interface contains a time-of-day clock; two dual digital-to-analog converters (DACS) (in all four outputs each of which generates a 0–10 V d.c. signal on command); an 8 low level (thermal e.m.f. < 1 μV) analog scanner to direct experiment voltages one at a time to a digital voltmeter; and a BCD input/output module.

The digital voltmeter (DVM) included in the interface is capable on its most sensitive range of reading voltages between +0.16 V and −0.16 V to microvolts. The DMV is remotely programmable and receives commands and transmits data via the BCD I/O module. A DVM rather than an analog-to-digital converter attached directly to the computer was chosen because of the greater flexibility and the possibility of later independence of the apparatus from the computer.

Details of the programming commands and philosophy are given in refs. 4 and 6. Here, suffice it to say that the four DAC's are used to generate voltages (described earlier in the text as "remotely originating") to specify required temperature, pressure and flow rates of nitrogen and oxygen. The analog scanner is used to select one of the voltages representing sample weight, furnace temperature, pressure, specified flow rate of N_2, specified flow rate of O_2, actual flow rate of N_2 or actual flow rate of O_2, and to direct that voltage to the DVM. The DVM range and options such as "filtered

* In no case does menton or usage of a commercially available instrument imply recommendation or endorsement by the National Bureau of Standards.

input" are set using the output portion of the BCD I/O module, and the unit is then triggered to take a reading of the input voltage. The result is then "unloaded", when it passes through the input portion of the BCD I/O module, is converted from parallel to serial form and is output through the controller module to the computer (or terminal if that is the mode of automation).

Computer and data storage

The computer used is a laboratory mini-computer, with a 32-K memory of 16 bit words. Communication using ASCII code is achieved through two programmable asynchronous single line communication interfaces which can be set to operate at character transmission speeds between 10 to 960 characters per sec inclusive. One line communicates with the interface at 120 characters per sec and the other is attached to a CRT computer terminal, operating at 960 characters/sec and serving as the console for the computer operator.

The computer also has a hexadecimal front panel which displays the output registers in both binary and hexadecimal and features a hexadecimal push-button mode of data entry rather than binary toggle switches. Hardwired multiply–divide (for integer operations) constitutes a recent improvement. Data and program storage is currently carried out using a four-drive flexible diskette ensemble. Our thermogravimetry experiment programs consist of several overlays written in FORTRAN. Program preparation is somewhat tedious because of the "slow" access time of the discs (about 3–6 lines per second), because of the "volatility" of the discs (susceptibility to being scratched, worn out by the drive head, etc.), the "volatility" of the disc drives (heads out of displacement, pressure pads lost or fouled by oxide), and because of the continual need for more storage (although each side of each disc will hold $\sim$ 3400 lines of 80 characters each). The disc containing the overlays and the disc used as a "scratch" unit to store data temporarily for transmission between overlays last for several weeks unless the disc drive itself fails as described above, when the disc usually becomes scratched. Fortunately, flexible diskettes are inexpensive; nonetheless, several backup copies must be kept of all important material. Diskettes are extremely convenient and desirable when compared with paper tape, magnetic cassettes and probably magnetic tapes or cartridges. They certainly have a place as a storage medium in continual rather than continuous use, and serve well as a mechanism of transferring information from one installation to another. However, for intense continuous use such as overlaid program structures, a hard-disc assembly is more appropriate. The hard disc holds $\sim$ 20 times the information on a diskette, is $\sim$ 6 times faster, supposedly less "volatile" (but more expensive), and is certainly much more resistant to wear. We plan to add one to the system in the near future.

The other mode of data output in our system is a printer–plotter. It uses an electrostatic paper-marking process and a wet development with a graphite suspension in a petroleum fraction solvent. Printing is satisfactorily fast at $\sim$ 500 lines per min, the plotting capability of the hardware (if not the software) produces respectable plots with a resolution of 0.01 in, and the pages fit in a letter size file. This is the normal

mode of outputting and storing the data and calculations which constitute a record of the experiment. A summary file of activation energies and temperatures, rates of weight loss and degrees of conversion at which they were determined is also kept on a flexible diskette and is routinely printed out at the ending of the listing of the experiment.

REFERENCES

1 J. H. Flynn and B. Dickens, *Thermochim. Acta*, 15 (1976) 1.
2 B. Dickens, W. J. Pummer and J. H. Flynn, in C. E. R. Jones and C. A. Cramers (Eds.), *Analytical Pyrolysis*, Elsevier, Amsterdam, 1976, p. 383.
3 B. Dickens and J. H. Flynn, in D. Dollimore (Ed.), *Proceedings of the First European Symposium on Thermal Analysis*, Heyden, 1976, p. 15.
4 B. Dickens, *Thermochim. Acta*, 29 (1979) 57.
5 B. Dickens, in preparation.
6 B. Dickens, *User's Manual for Factor-jump Thermogravimetry Apparatus and Associated Computer Programs, including a General Plotting Program*, National Bureau of Standards Internal Report, 1978.
7 E. I. Lowe and A. E. Hidden, *Computer Control in Process Industries*, Peregrinus Verlag, Starnberg, B.R.D., 1971, p. 23.
8 J. G. Ziegler and N. B. Nichols, *Trans. Am. Soc. Mech. Eng.*, 64 (1942) 759.
9 C. H. Popenoe and M. S. Campbell, *Nat. Bur. Stand. (U.S.), Tech. Note 790*, 1973.